Hindawi
International Journal of Chemical Engineering
Volume 2019, Article ID 8621951, 12 pages
https://doi.org/10.1155/2019/8621951

Research Article

Activated Carbon from Prickly Pear Seed Cake: Optimization of Preparation Conditions Using Experimental Design and Its Application in Dye Removal

Y. El Maguana,[1] **N. Elhadiri**,[1] **M. Bouchdoug**,[1] **M. Benchanaa**,[1] **and A. Jaouad**[2]

[1]*Research Laboratory on Materials Reactivity and Process Optimization «REMATOP», Department of Chemistry, Faculty of Science Semlalia, Cadi Ayyad University, B.P. 2390 Marrakech, Morocco*
[2]*Equipe de Recherche d'Innovation et de Développement Durable en Chimie Verte «ERIDDECV», Department of Chemistry, Faculty of Science Semlalia, Cadi Ayyad University, BP 2390 Marrakesh, Morocco*

Correspondence should be addressed to Y. El Maguana; youssefelmaguana@gmail.com

Received 28 August 2018; Revised 2 January 2019; Accepted 25 February 2019; Published 1 April 2019

Academic Editor: Eric Guibal

In the present study, the experimental design method was used to optimize the preparation conditions of an activated carbon from prickly pear seed cake by phosphoric acid activation. The parameters studied include impregnation ratio, carbonization temperature, and carbonization time. The optimal conditions for the preparation of the activated carbon with high adsorption capacity for methylene blue were identified to be an impregnation ratio of 2.9, carbonization temperature of 541°C, and carbonization time of 88 min. The obtained activated carbon was characterized by SEM/EDX, FTIR, pH_{pzc}, and its capacity to adsorb methylene blue. FTIR analysis and pH_{PZC} showed the acidic character of the activated carbon surface. The adsorption capacity of the optimal activated carbon was found to be 260 mg·g^{-1} for methylene blue. The adsorption equilibrium of methylene blue was well explained by the pseudo-second-order model and Freundlich isotherm. Furthermore, the performance of the produced activated carbon was examined by the methyl orange removal.

1. Introduction

The generation of large quantities of the agricultural byproducts and industrial wastes has become a crucial problem in many countries all around the world, particularly in countries where the environmental concerns have been raised in the last few years. Thus, the scientific community has become increasingly concerned with the waste treatment by developing innovative chemicals and materials. The utilization of the remaining residues has a positive impact on reducing solid wastes, on the production of low-cost materials with high added value, and on the protection of the environment [1]. Consequently, the organic solid wastes are valorized toward different value-added products: animal feeding [2, 3], composting-fertilizer [4, 5], energy [6, 7], biofuels [8, 9], activated carbon [10, 11], etc.

The activated carbon is defined as a carbonaceous solid characterized by its large specific surface and its high adsorption capacity towards gaseous or dissolved compounds. It is extensively used in a variety of applications such as gas purification, water purification, metal extraction, gold recovery, medicine, sewage treatment, air filters in filter masks, filters in compressed air, and so on [1, 12, 13]. Thus, activated carbons have been prepared from walnut shells [14], olive stones and sugar cane bagasse [15, 16], coconut shell [17], wood sawdust [18], argan shells [19], etc.

Activated carbon can be prepared, by physical or chemical activation, from different organic materials rich in carbon [12]. The physical activation comprises two steps that starts with the carbonization of the precursor followed by the activation of the resulting material in an oxidizing atmosphere such as carbon dioxide, steam, or a combination of both at the elevated temperature range of 800°C to 1100°C [20]. On the other hand, the chemical activation comprises one step that involves the impregnation of the raw material with an activating agent such as KOH, $ZnCl_2$, and H_3PO_4,

and after the carbonization of the impregnated material at the temperature range of 400°C to 600°C and washing, the final activated carbon is produced [13]. The chemical activation offers several advantages: one step process, low energy cost, high yield in carbon, and efficient activated carbon with mixed porosity [12, 21].

The prickly pear cactus is native to the United States, Mexico, and South America, but it grows as well in other areas, including Africa, Australia, and the Mediterranean region. It is specie of plant that has the ability to live in arid and semiarid zones with a small amount of water. The prickly pear fruit seeds represent a source of good quality edible oil, which can be utilized in nutritional, cosmetic, perfumery, and pharmaceutical industries because it presents higher concentration of phenolic compounds and essential fatty acids (linoleic acid or omega-6). This oil offers nutritional and antioxidant properties such as nourishing, antiaging, protection against certain types of cancer, etc. The prickly pear seed oil requires between 800 kg and 1000 kg of prickly pear fruit to extract 1 liter of oil. Therefore, a considerable amount of waste seeds (prickly pear seed cake) was generated during the oil extraction [22–24].

The aim of this work is to prepare an activated carbon from prickly pear seed cake by chemical activation using phosphoric acid (H_3PO_4) as a chemical activator for the dye removal from aqueous solution. H_3PO_4 has been used as an activator in several researches for the preparation of the activated carbons from various agricultural byproducts [25–30]. H_3PO_4 minimizes the formation of tars and other liquids that could clog up the pores of the activated carbons [20]. The response surface methodology was used to study the influence of the impregnation ratio, the carbonization temperature, and the carbonization time which are the most influential factors on the characteristics of activated carbons on the adsorption of methylene blue (MB) and to determine the optimal conditions of the preparation [25, 26, 31, 32]. The activated carbon prepared at the optimal conditions was characterized by different methods to determine the morphological features, the surface functions, and the point of zero charge. The efficiency of the obtained activated carbon was tested by the removal of methyl orange from aqueous solution.

2. Materials and Methods

2.1. Preparation of Activated Carbons. The prickly pear seed cake used in this study was brought from a prickly pear seed oil processing unit in the region of Oujda, Morocco. It was dried at 110°C for 24 h, crushed, and sieved to obtain particles size less than 200 μm. The raw material was activated using phosphoric acid. Thus, 5 g of the prickly pear seed cake was impregnated by 50 mL of phosphoric acid solution (85%) to give an impregnation ratio between 1 and 3. The impregnation ratio was determined as the mass ratio of the phosphoric acid to the precursor (impregnation ratio = mass of phosphoric acid/mass of precursor). The mixture was stirred at 60°C for 1 h and dried at 110°C for 12 h to remove the residual water. The dried mixture was put in a tubular furnace (Carbolite Ltd, UK) and heated at a rate of 20°C min^{-1} and held at different carbonization temperatures between 400 and 600°C during desired carbonization time varied between 1 h and 2 h. The carbonization is carried out with nitrogen in a reactor of stainless steel with a flow of 200 $cm^3 \cdot min^{-1}$. After cooling to room temperature, the produced activated carbon was then repeatedly washed with distilled water until the pH of the washing solution reached a constant value (between 6 and 7) and dried at 110°C overnight. Finally, the product was ground (granulometry less than 100 μm) and stored for later experimental uses.

2.2. Adsorption Tests. The adsorption capacity of the prepared activated carbons was determined by performing batch mode adsorption. The adsorption amounts were determined by adding 0.01 g of activated carbon samples to flasks containing 100 cm^3 of adsorbate solution. These flasks were kept in a shaker of 180 rpm at room temperature (20°C). After adsorption, the residual concentration of methylene blue and methyl orange was determined by the spectrophotometric method (UV-3100PC Spectrophotometer) at 664 nm and 462 nm, respectively. Methylene blue was chosen in the optimization step to study the mesopores of the activated carbons and also serves as a model compound for adsorption of organic contaminants from aqueous solution [12].

The amount of adsorption q_e at equilibrium is defined as the amount of adsorbate per gram of adsorbent (in $mg \cdot g^{-1}$) and was calculated by the following equation:

$$q_e = \frac{C_0 - C_e}{m} \times V, \quad (1)$$

where C_0 and C_e (in $mg \cdot L^{-1}$) are the initial and equilibrium concentrations in aqueous solution, respectively; V (L) is the volume of the solution; and m (g) is the mass of the adsorbent.

2.3. Activated Carbon Yield. The yield of the activated carbon is defined as the ratio of the mass of the activated carbon obtained after activation, washing, and drying to the mass of the precursor. It was calculated based on the following equation:

$$\text{yield}\,(\%) = \frac{m}{m_0} \times 100, \quad (2)$$

where m (g) is the mass of the activated carbon produced and m_0 (g) is the mass of the precursor.

2.4. Characterization Techniques. Scanning electron microscopy coupled with energy dispersive x-ray spectroscopy (SEM/EDX) was used to examine the morphology and the development of porosity of activated carbon prepared under the optimal conditions as well as to determine its elemental composition using TESCAN VEGA3–EDAX instrument with an accelerating voltage of 20 kV. The surface functional groups of the optimal activated carbon were carried out by Fourier transformed infrared (FTIR) spectroscopy on a

Nicolet 5700 spectrometer in the scanning range of 4000 to 400 cm^{-1} (64 scans, at a resolution of 4 cm^{-1}).

The pH at point of zero charge (pH_{pzc}) corresponds to the pH at which the surface net charge of the adsorbent is zero. It was determined according to the method described by Baccar et al. [33]. 50 mL of 0.01 M NaCl solution was taken and its initial pH was adjusted between 2 and 10 using 0.1 M of HCl and NaOH with a pH meter. Then, 100 mg of adsorbent was added to each flask. These flasks were kept for 48 h and the final pH of the solutions was measured. The pH_{pzc} of adsorbent was identified by the intersection of the curves, $pH_f = f(pH_i)$.

2.5. Response Surface Methodology. The response surface methodology is a mathematical and statistical technique useful for modeling and analyzing problems or responses affected by different factors [12]. It was used to optimize the impregnation ratio (U_1), the carbonization temperature (U_2), and the carbonization time (U_3) in the experimental domains described in Table 1. The response analyzed was the adsorption of methylene blue. It was related to the impregnation ratio, the carbonization temperature, and the carbonization time by a model is given as follows:

$$Y = b_0 + b_1X_1 + b_2X_2 + b_3X_3 + b_{11}X_2^2 + b_{33}X_3^2 + b_{12}X_1X_2 + b_{13}X_1X_3 + b_{23}X_2X_3, \quad (3)$$

where Y is the response (methylene blue adsorption). X_1, X_2, and X_3 are the coded variables related to the impregnation ratio (U_1), carbonization temperature (U_2), and carbonization time (U_3), respectively. b_0 is a constant, b_1 represents the weight of impregnation ratio, b_2 represents the weight of carbonization temperature, and b_3 represents the weight of carbonization time. b_{12} is the interaction effect between the impregnation ratio and the carbonization temperature, b_{13} is the interaction effect between the impregnation ratio and the carbonization time, and b_{23} is the interaction effect between the carbonization temperature and the carbonization time. b_{11}, b_{22}, and b_{33} can be regarded as a curve shape parameter.

In the present study, the Doehlert design was applied using NEMROD software (New Efficient Methodology for Research using Optimal Design) for generating the experimental design, estimating the coefficients, and analyzing the results. It is worth noting that this design permits to represent the response studied in all the experimental domains with a minimum number of experiments for later predication of response in each point of the domain [1].

3. Results and Discussion

3.1. Response Analysis and Interpretation. Table 2 presents the Doehlert experimental design and experimental results. The experimental domain center was repeated three times in order to validate the experimental error and to test the reproducibility of the response [1, 34]. Estimated values of coefficients for the response methylene blue adsorption (Y) are given in Table 3.

The amount of adsorption of methylene blue on the activated carbon, given in Table 2, varies between 56.07 and 234.81 $mg \cdot g^{-1}$. As seen from the estimated values of coefficients (Table 3), the methylene blue adsorption is influenced by the impregnation ratio ($b_1 = 46.33$) and carbonization temperature ($b_2 = 13.99$) with positive impact and by carbonization time ($b_3 = -45.30$) with negative impact. The impregnation ratio and carbonization time seem to be the more influential factors. Moreover, one significant interaction exists between impregnation ratio and carbonization temperature ($b_{12} = 61.83$). The increase in impregnation ratio produces a significant increase in the adsorption of methylene blue (Figures 1(a) and 1(b)). The increase of the methylene blue removal could be due to the development of the porous structure and to the increase in P-content [12]. The same results were also observed by Tounsadi et al. [27]. Figures 1(b) and 1(c) show that the increase in the calcination time induces a major reduction in the adsorption of methylene blue. Furthermore, it can be observed from Figures 1(a) and 1(c) that the best adsorption capacity is obtained in the center of the experimental domain of the temperature (500°C). These results conform to those obtained by Patnukao et al. [35]. Thus, it is necessary to operate at high level of impregnation ratio and at low level of carbonization time and in the center of the domain of interest to have a better adsorption capacity.

Table 1: Experimental domains for the Doehlert experimental design.

Factors	Undimensional variables	Experimental domain
U_1: impregnation ratio	X_1	1 to 3
U_2: carbonization temperature (°C)	X_2	400 to 600
U_3: carbonization time (min)	X_3	60 to 120

The adsorption of methylene blue Y_2 can be described as follows:

$$Y = 160.467 + 46.33X_1 + 13.99X_2 - 45.30X_3 + 53.51X_1^2 - 45.01X_2^2 - 13.26X_3^2 + 61.83X_1X_2. \quad (4)$$

3.2. Optimization. The impregnation ratio, carbonization temperature, and carbonization time are optimized simultaneously using the desirability function included in the Nemrodw software to determine the optimal conditions for the preparation of activated carbon with high adsorption capacity for methylene blue. The desirability function varies in the interval [0,1], the value 1 corresponds to the maximum satisfaction (desired value), and 0 corresponds to an unacceptable response [36, 37]. The maximum of the function gives the best global compromise for the response in the studied domains and corresponds to the optimal experimental conditions. All the information and results of the multicriteria optimization are given in Table 4. After the calculation by the Nemrodw software, the optimal point which corresponds to the maximum of the global desirability function is found for an impregnation ratio of 2.9, carbonization temperature of 541°C, and carbonization time of

Table 2: Doehlert experimental design, experimental conditions, and experimental results.

Exp. No.	Doehlert experimental design			Experimental conditions			Exp. response
	X_1	X_2	X_3	U_1	U_2 °C	U_3 Min	Y mg·g^{-1}
1	1.0000	0.0000	0.0000	3.00	500.00	90.00	234.81
2	−1.0000	0.0000	0.0000	1.00	500.00	90.00	193.15
3	0.5000	0.8660	0.0000	2.50	586.60	90.00	190.42
4	−0.5000	−0.8660	0.0000	1.50	413.40	90.00	143.30
5	0.5000	−0.8660	0.0000	2.50	413.40	90.00	151.09
6	−0.5000	0.8660	0.0000	1.50	586.60	90.00	75.54
7	0.5000	0.2887	0.8165	2.50	528.87	114.50	191.59
8	−0.5000	−0.2887	−0.8165	1.50	471.13	65.50	136.68
9	0.5000	−0.2887	−0.8165	2.50	471.13	65.50	210.28
10	0.0000	0.5774	−0.8165	2.00	557.74	65.50	223.13
11	−0.5000	0.2887	0.8165	1.50	528.87	114.50	100.47
12	0.0000	−0.5774	0.8165	2.00	442.26	114.50	56.07
13	0.0000	0.0000	0.0000	2.00	500.00	90.00	160.53
14	0.0000	0.0000	0.0000	2.00	500.00	90.00	158.10
15	0.0000	0.0000	0.0000	2.00	500.00	90.00	162.77

Table 3: Estimated values of coefficients for response Y.

No.	Coefficient	Significance (%)
b0	160.467	0.0118***
b1	46.33	0.0438***
b2	13.99	0.469**
b3	−45.30	0.0454***
b11	53.51	0.0972***
b22	−45.01	0.137**
b33	−13.26	1.90*
b12	61.83	0.116**
b13	−11.13	6.4
b23	−6.33	17.1

***Statistically significant at the <99.99% level. **Statistically significant at the 99% level. *Statistically significant at the 95% level.

88 min. At these conditions, the predicted value of methylene blue adsorption calculated from the model was 271.56 mg·g^{-1}. In order to validate the model, three activated carbon samples were prepared under the optimal conditions. The methylene blue adsorption of the obtained adsorbent was 260 mg·g^{-1}, which is higher than that of the raw prickly pear seed cake (23.81 mg·g^{-1}). It is clear from these results that the chemical activation and the carbonization increase the adsorption capacity of methylene blue. The difference between the experiment and the predicted values is very lower, which confirm the good accuracy of the model. The yield of the activated carbon prepared under the optimal conditions was 56.48%. The methylene blue adsorption capacity of the activated carbon obtained in this study is comparable to or greater than that of the activated carbons found in literature [38–43].

3.3. Characterization of the Optimal Activated Carbon. Figure 2 shows SEM micrographs of raw prickly pear seed cake and optimal activated carbon. It illustrates that the prickly pear seed cake surface was modified by chemical activation; the pores are clearly identified in the surface of the prepared activated carbon, which seems to be the main factor that resulted in the higher adsorption capacity of the resulting activated carbon. The results of the elemental analysis of the activated carbon using EDX (Figure 3) indicate that the major elements present in the prickly pear seed cake are carbon (57.1%) and oxygen (42.5%). The optimal activated carbon contains higher amounts of carbon (79.1%) and oxygen (19.8%) and less amount of phosphorus (1.1%).

Figure 4 corresponds to the FTIR spectrum of activated carbon prepared under the optimum conditions. The band located at around 3425 cm^{-1} was attributed to O–H stretching vibrations in hydroxyl groups [22]. The band appearing at 2380 cm^{-1} was ascribed to P–OH stretching vibrations [44]. The band at 1627 cm^{-1} could be attributed to the C=C stretching in aromatics [45]. According to Barka et al. [22] and Prahas et al. [25], the peak at 1170 cm^{-1} is indicative of the stretching vibrations of P=O, P=OOH, and O–C in P–O–C and the peak at 1080 cm^{-1} can be ascribed to the ionized linkage P^+–O^- in acid phosphate esters and to symmetrical vibrations in a chain of P–O–P. The peak at 521 cm^{-1} could be assigned to P–O stretching vibrations and/or to aromatic structures [26, 44]. These results indicate that the activated carbon contains a variety of functional groups, which have enhanced the adsorption capacity of the solid.

The pH_{PZC} value of the activated carbon obtained under optimal conditions was 3.8 (Figure 5). When the pH is lower than 3.8, the surface of the activated carbon gets positively charged and the surface is negatively charged in pH values higher than 3.8. Therefore, the activated carbon produced from prickly pear seed cake at the optimal conditions has an acidic characteristic, which is in agreement with FTIR analysis which indicates the presence of oxygen functions on the surface of the activated carbon. Consequently, in aqueous solution (pH 6–7), the activated carbon surface acquires a negative charge, which is the result of the interactions between the ions in the solution and the functional groups on the surface of the adsorbent, which will promote the adsorption of positively charged compounds.

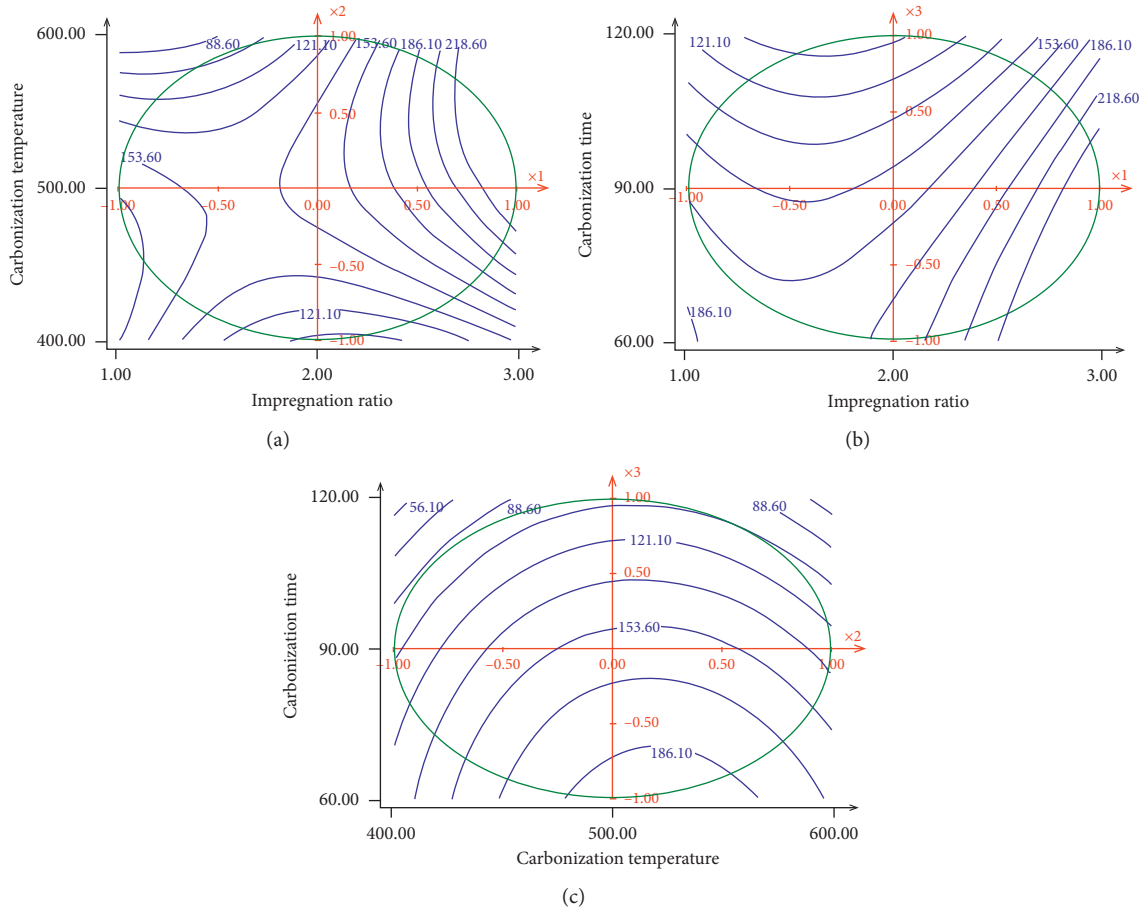

Figure 1: Variation of the methylene blue adsorption as a function of (a) impregnation ratio and carbonization temperature, (b) impregnation ratio and carbonization time, and (c) carbonization temperature and carbonization time.

Table 4: Characteristics of maximum for response Y.

Response	Lower limit	Target value	Weight	d_{min} (%)	d_{max} (%)	Cal. value	Exp. value
Y = MB adsorption (mg·g^{-1})	180	280	1	88.11	92.78	271.56	260

d: desirability of response Y; d_{min}: minimal desirability of response Y; d_{max}: maximal desirability of response Y; Cal. value: calculated value; Exp. value: experimental value.

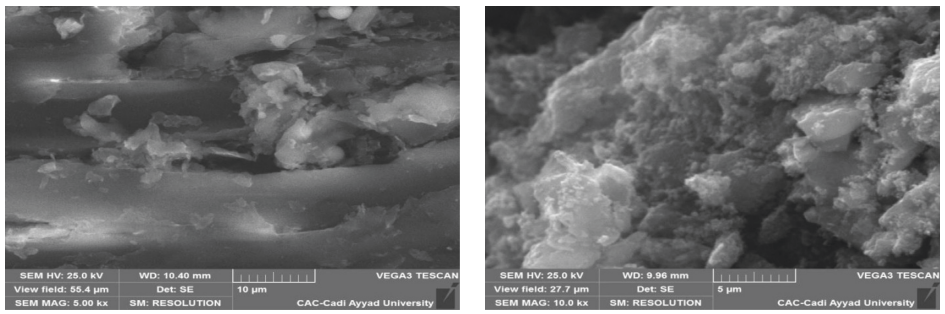

(a) (b)

Figure 2: SEM of (a) raw prickly pear seed cake and (b) optimal activated carbon.

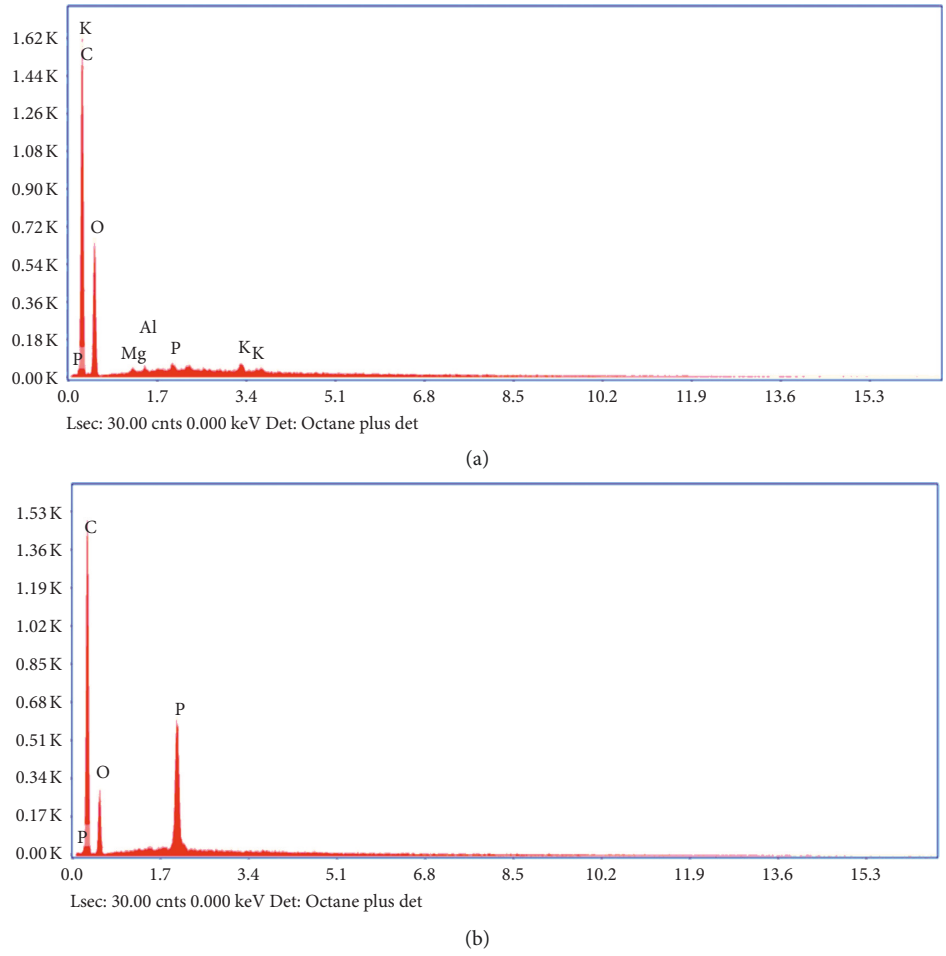

Figure 3: EDX of (a) raw prickly pear seed cake and (b) optimal activated carbon.

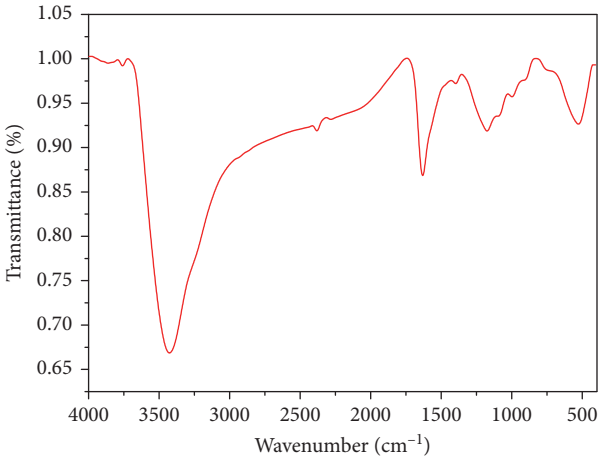

Figure 4: FTIR spectra of the activated carbon prepared at the optimal conditions.

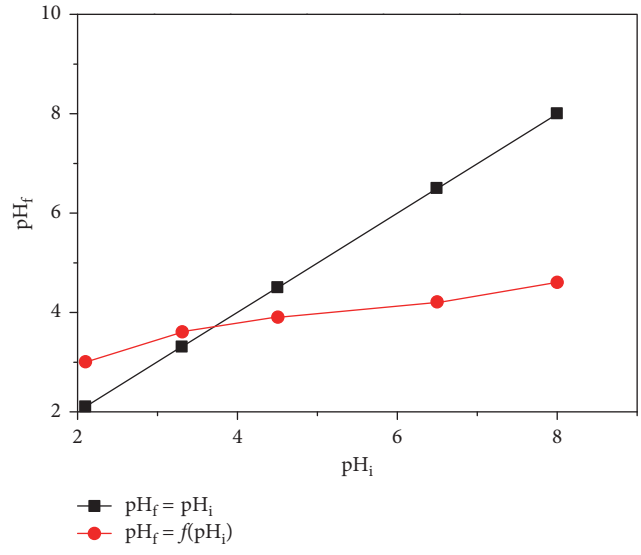

Figure 5: pH$_{pzc}$ of the activated carbon prepared at the optimal conditions.

3.4. Study of the Influence of Some Factors on the Removal of Methylene Blue

3.4.1. Effect of Contact Time. The amount of the adsorption of methylene blue on the activated carbon prepared at the optimal conditions was presented as a function of time in Figure 6. It shows that the adsorbed amount increased with contact time at the initial stage of adsorption and almost remained constant at 180 min. The adsorption

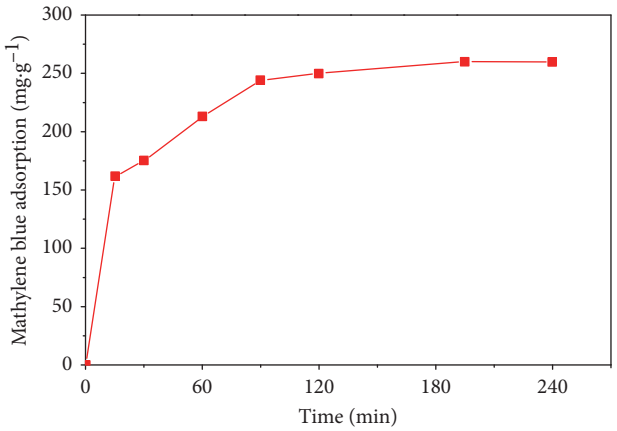

Figure 6: Effect of contact time on the methylene blue adsorption (adsorbent dose = 0.2 g L^{-1}; C_0 = 200 mg L^{-1}; T = 20°C; pH ~ 7).

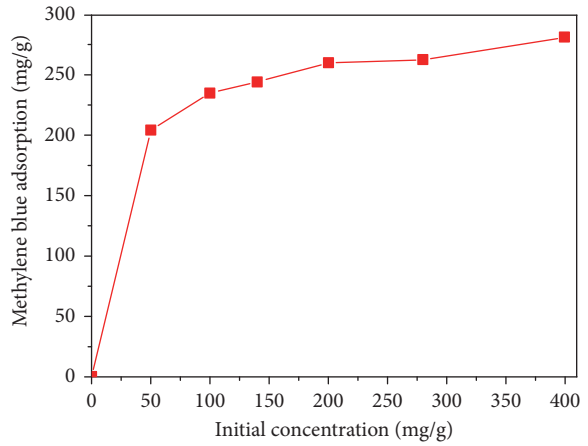

Figure 7: Effect of initial methylene blue concentration (contact time = 180 min; adsorbent dose = 0.2 g L^{-1}; T = 20°C; pH ~ 7).

process of methylene blue was rapid at the beginning of the process due to the availability of active sites on the exterior surfaces, and after the saturation of those active sites, the methylene blue entered to the pores of the adsorbent with a slower rate to reach the equilibrium time [46]. The amount of methylene blue removed by the optimal adsorbent at the equilibrium time (180 min) was 260 mg·g^{-1}.

3.4.2. Effect of Initial Methylene Blue Concentration. As seen from Figure 7, the increase in initial methylene blue concentration produces an increase in adsorption of methylene blue. This observation can be explained by the fact that when the concentration gradient between the aqueous solution and the solid phase increases, the diffusion rate increases [36]. Moreover, the increase in the initial concentration increases the contact probability between methylene blue and the activated carbon [47].

3.4.3. Effect of Initial pH Solution. The solution pH has been identified as an important operating parameter governing the adsorption of dyes onto the adsorbents because the solution pH can affect the surface charge of the adsorbent and dye molecules. Figure 8 illustrates the adsorption capacity of the activated carbon as a function of solution pH. As can be seen from Figure 8, the adsorption capacity of the activated carbon increases with increasing solution pH. This can be explained by the increase of negatively charged sites on the surface of the activated carbon, which favors the electrostatic attraction between the positively charged dye and the activated carbon. It should be noted that the point of zero charge of the activated carbon was 3.8, implying that the surface of the activated carbon is negatively charged at pH > 3.8, which favors the adsorption of the methylene blue as a cationic dye. At pH < 3.8, the surface of the activated carbon is positively charged and the methylene blue adsorption is inhibited, due to an electrostatic repulsion between the methylene blue and the positively charged surface.

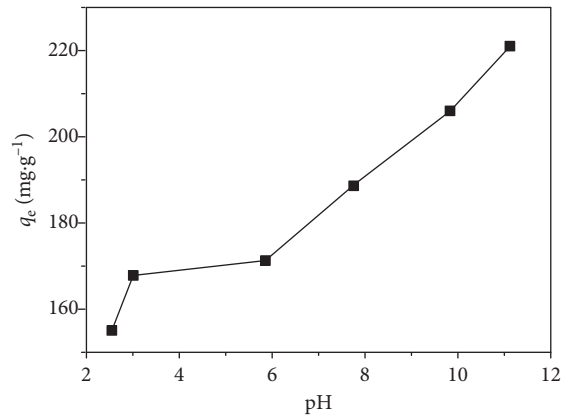

Figure 8: Effect of pH on the adsorption of methylene blue on the optimal activated carbon (C_0 = 50 mg L^{-1}; contact time = 180 min; adsorbent dose = 0.2 g L^{-1}; T = 15°C).

3.5. Adsorption Kinetics Models. In order to predict the mechanism of the adsorption process of methylene blue onto the adsorbent prepared under optimal conditions, the pseudo-first-order (equation (5)), pseudo-second-order (equation (6)), and intraparticle diffusion (equation (7)) models were tested to fit the experimental data. We employed pseudo-first-order and pseudo-second-order models in their nonlinear forms to determine the kinetic parameters because, in this way, the kinetic parameters are predicted better than in the linearized forms of these models [48]:

$$q_t = q_e\left(1 - e^{-k_1 t}\right), \tag{5}$$

$$q_t = \frac{k_2 q_e^2 t}{1 + k_2 q_e t}, \tag{6}$$

$$q_t = k_{id} t^{1/2} + c, \tag{7}$$

where q_e (mg·g^{-1}) is the adsorption amounts at equilibrium, q_t (mg·g^{-1}) is the adsorption amounts at time t (min); k_1 (min^{-1}), k_2 (g·mg^{-1}·min^{-1}), and k_{id} (mg·g^{-1}·min$^{-1/2}$) are the

adsorption rate constants of pseudo-first-order, pseudo-second-order, and intraparticle diffusion models, respectively; and c is a constant related to the thickness of the boundary layer.

The validity of these models was evaluated by the coefficient of regression R^2 and by the normalized standard deviation Δq (%), defined as follows:

$$\Delta q(\%) = 100\sqrt{\frac{\sum\left[\left(q_{\text{exp}} - q_{\text{cal}}\right)/q_{\text{exp}}\right]^2}{N-1}}, \tag{8}$$

where q_{exp} and q_{cal} are the experimental and calculated equilibrium adsorption capacity value, respectively, and N is the number of data points.

The calculated kinetic parameters of pseudo-first order and pseudo-second order are summarized in Table 5. The results (Table 5 and Figure 9) showed that the fitting data to the pseudo-second-order model gave the higher R^2 value and lower Δq value than the pseudo-first-order model. Additionally, the adsorption capacity calculated by the pseudo-second order is closer to the experimental value. Therefore, the pseudo-second-order model can describe the adsorption process of methylene blue on the obtained activated carbon. This result suggests that the boundary layer resistance was not the rate-limiting step [22].

The plot of the intraparticle diffusion model is shown in Figure 10. The plot is multilinear during the time range, having three linear segments, which indicated that intraparticle diffusion was not the only rate-limiting mechanism in the adsorption process. The first stage is attributed to the diffusion of methylene blue through the solution to the external surface of the adsorbent. The second portion was ascribed to the intraparticle diffusion. The third portion is attributed to the final equilibrium stage for which the intraparticle diffusion starts to slow down due to the decrease in the methylene blue concentration [22, 49].

3.6. Adsorption Isotherms. The adsorption isotherm describes the interaction between the adsorbate molecules and the adsorbents when the system reaches the equilibrium [17, 18]. The experimental data were fitted to the Langmuir and Freundlich models to find which one can be used to describe the adsorption process of methylene blue on the surface of activated carbon. The Langmuir isotherm is based on the assumption of monolayer adsorption on a homogenous surface without interaction between adsorbates [14, 50], while the Freundlich isotherm assumes the multilayer adsorption on heterogeneous surface [51]. We employed the Langmuir isotherm and Freundlich isotherm in their nonlinear forms given by equations (9) and (10) respectively. The theoretical model that most appropriately describes the experimental data was chosen from the correlation coefficient R^2 and the normalized standard deviation Δq:

$$q_{\text{e}} = \frac{q_{\text{m}} \cdot K_{\text{L}} \cdot C_{\text{e}}}{1 + K_{\text{L}} \cdot C_{\text{e}}}, \tag{9}$$

$$q_{\text{e}} = K_{\text{F}} C_{\text{e}}^{1/n}, \tag{10}$$

where C_{e} is the equilibrium concentration of the adsorbate, q_{e} is the amount of adsorption at the equilibrium, q_{m} is the monolayer adsorption capacity, n is the Freundlich intensity constant, and K_{L} and K_{F} are the Langmuir and Freundlich constants, respectively.

The adsorption isotherm for methylene blue onto activated carbon is shown in Figure 11, and the calculated parameters are listed in Table 6. It can be seen from Table 6 that the adsorption process is well fitted to both Langmuir ($R^2 = 0.993$) and Freundlich ($R^2 = 0.999$) models. The standard deviation of the Langmuir isotherm is higher than that of the Freundlich isotherm. Therefore, the adsorption process can be described more appropriately by the Freundlich isotherm, which indicates the multilayer adsorption on the heterogeneous surface with a different energy distribution [49]. The $1/n$ value which is between 0 and 1 indicates the favorable adsorption of methylene blue on the activated carbon [41, 52].

3.7. Thermodynamic Study. The thermodynamic parameters, including the free Gibbs energy (ΔG°), enthalpy (ΔH°), and entropy (ΔS°), were calculated using equations (11) and (12) to evaluate thermodynamic feasibility of the adsorption processes:

$$\Delta G^\circ = -RT\ \ln\left(K_{\text{e}}^0\right), \tag{11}$$

$$\ln\left(K_{\text{e}}^0\right) = -\frac{\Delta H^\circ}{R} \cdot \frac{1}{T} + \frac{\Delta S^\circ}{R}, \tag{12}$$

where R is the universal gas constant ($8.314\ \text{J}\cdot\text{K}^{-1}\ \text{mol}^{-1}$), T is the absolute temperature (Kelvin), and K_{e}^0 is the thermodynamic equilibrium constant.

The thermodynamic parameters were obtained by performing the isotherm of adsorption at different temperatures and making the nonlinear fitting of the isotherms. From the best fitted model (usually K_{L} of Langmuir, K_{S} of Sips, and K_{g} of Liu), the equilibrium constant K is obtained. It could be obtained as dimensionless by multiplying the value of K (expressed in $\text{L}\cdot\text{mg}^{-1}$) by the molecular weight of adsorbate (methylene blue; $319.85\ \text{g}\cdot\text{mol}^{-1}$), 1000, and then the unitary standard concentration of the adsorbate ($1\ \text{mol}\cdot\text{L}^{-1}$) and making the division by the activity coefficient γ (equation (13)) [53]. To consider that the activity coefficient is unitary (equal to 1), we considered that the adsorbate solution is very diluted:

$$K_{\text{e}}^0 = \frac{\left(1000 \cdot K_L \cdot \text{molecular weight of adsorbate}\right) \cdot [\text{adsorbate}]^\circ}{\gamma}. \tag{13}$$

The values of ΔH° and ΔS° can be determined from the slope and intercept of the plot of $\ln(\text{K}_{\text{e}}^0)$ versus $1/T$. The values of ΔG°, ΔH°, and ΔS° were calculated and are listed in Table 7. The negative values of ΔG° indicate the feasibility and spontaneous of the adsorption processes of methylene blue onto optimal activated carbon. The positive values of ΔH° and ΔS° indicated the endothermic nature of the adsorption process and the increased randomness at the solid-

Table 5: Pseudo-first-order and pseudo-second-order kinetics parameters.

$q_{e,exp}$ (mg g^{-1})	Pseudo-first order				Pseudo-second order			
	$q_{e,cal}$ (mg g^{-1})	k_1 (min^{-1})	R^2	Δq (%)	$q_{e,cal}$ (mg g^{-1})	k_2 (g·mg^{-1}·min^{-1})	R^2	Δq (%)
260	245.50	51.1 10^{-3}	0.95	9.9	268.60	0.28 10^{-3}	0.99	3.8

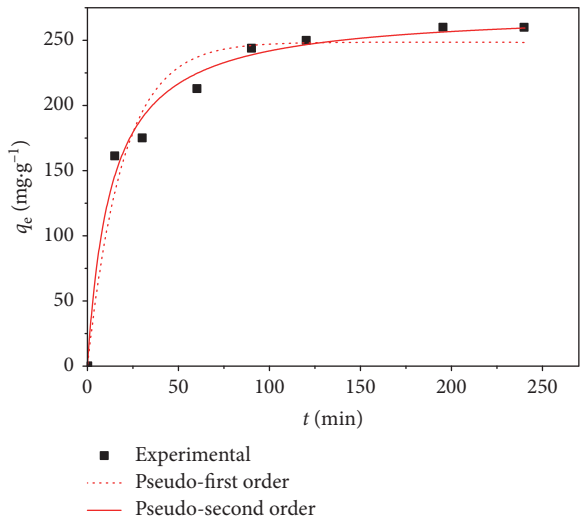

Figure 9: Nonlinear fits of pseudo-first-order and pseudo-second-order kinetics for methylene blue adsorption onto activated carbon.

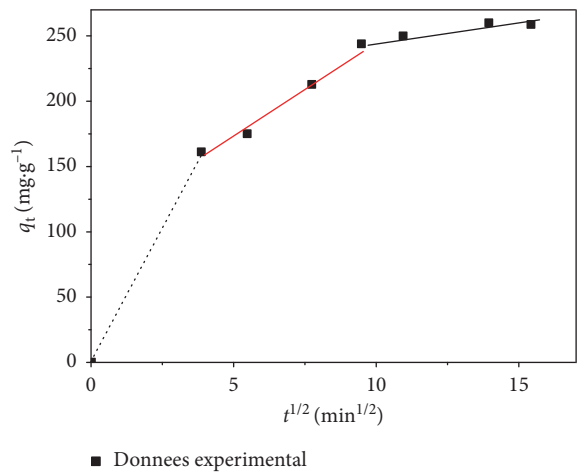

Figure 10: Plot of the intraparticle diffusion model for methylene blue adsorption onto activated carbon.

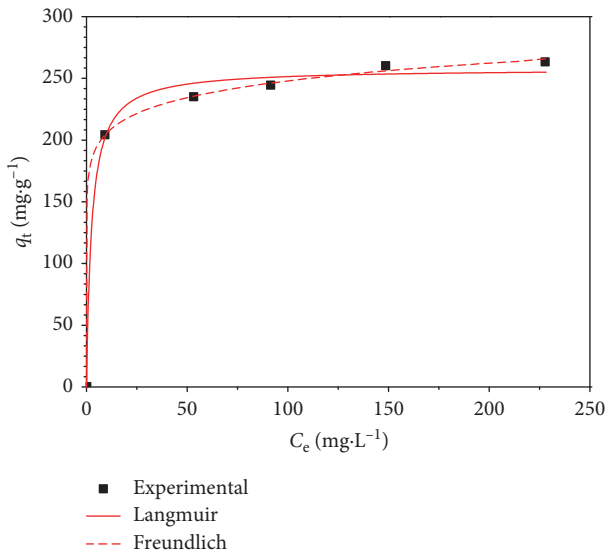

Figure 11: Nonlinear fits of the Langmuir and Freundlich isotherms for methylene blue adsorption onto activated carbon.

Table 6: Langmuir and Freundlich isotherm parameters at 20°C.

Langmuir	Freundlich
$q_m = 257.86$ mg·g^{-1}	$K_F = 169.85$ ((mg·g^{-1}) (L·mg^{-1})$^{1/n}$)
$K_L = 0.3936$ L·mg^{-1}	$n = 12.31$
$R^2 = 0.993$	$R^2 = 0.999$
$\Delta q = 4.22$	$\Delta q = 1.23$

Table 7: Thermodynamic parameters for MB adsorption on optimal activated carbon.

Temperature (K)	ΔG° (kJ·mol^{-1})	ΔH° (kJ·mol^{-1})	ΔS° (J·K^{-1}·mol^{-1})
293	−33.96	9.66	82.64
303	−34.54		
313	−35.62		

solution interface during the fixation of the methylene blue on the active sites of the studied adsorbent. The value of ΔH° is smaller than 40 kJ·mol^{-1}, which reveals that the adsorption of methylene blue onto activated carbon was a physisorption process in nature.

3.8. Application: Removal of Methyl Orange from the Aqueous Solution. The removal of methyl orange (MO) by the optimal activated carbon was studied as a function of time, adsorbent dose, and initial concentration. From Figure 12, the time required to reach the equilibrium was 120 min. Figure 13 shows the effect of the adsorbent dose, ranging from 0.2 to 2 g·L^{-1}, on the removal of methyl orange. It can be seen that the methyl orange uptake increased with increasing the adsorbent dose and reached almost 100 % at 2 g·L^{-1}. This is due to the increase in the number of the available adsorption sites for the adsorption of methyl orange. The removal amount of methyl orange at equilibrium time increased, respectively, from 19.83 to 336.12 mg·g^{-1} with an increase in the initial dye concentration from 20 to 600 mg·L^{-1} (Figure 14). These results demonstrated that the obtained activated carbon is effective for removing dyes from aqueous solution.

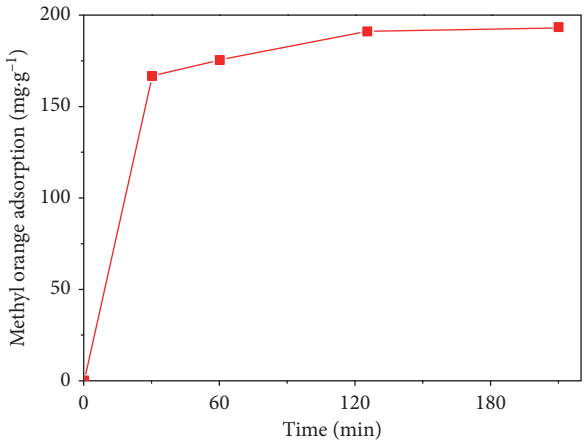

Figure 12: Effect of contact time on the methyl orange adsorption (adsorbent dose = 0.2 g·L^{-1}; C_0 = 100 mg·L^{-1}; T = 20°C; pH ~ 7).

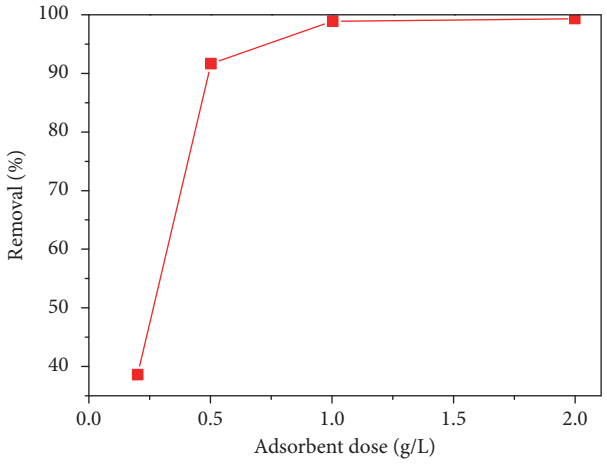

Figure 13: Effect of adsorbent dose on the methyl orange adsorption (contact time = 120 min; C_0 = 100 mg·L^{-1}; T = 20°C; pH ~ 7).

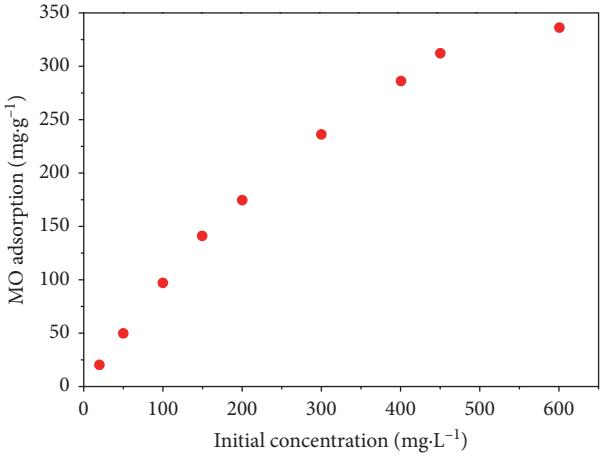

Figure 14: Effect of initial methyl orange concentration on the methyl orange adsorption (contact time = 120 min; adsorbent dose = 1 g·L^{-1}; T = 20°C; pH ~ 7).

4. Conclusion

The results of the present study showed that the prickly pear seed cake is a suitable precursor for the production of adequate activated carbon for dye removal from industrial effluents. The optimal conditions for the preparation of the activated carbon with high adsorption capacity for methylene blue were identified to be an impregnation ratio of 2.9, carbonization temperature of 541°C, and carbonization time of 88 min. At these conditions, the yield in carbon and the adsorption of methylene blue were 56.48% and 260 mg·g^{-1}, respectively. FTIR analysis indicated the presence of various functional groups (oxygen functions and phosphorus compounds) on the surface of the obtained activated carbon, which gave the adsorbent an acidic surface (pH_{PZC} = 3.8). The adsorption of methylene blue was described by the pseudo-second-order model and Freundlich isotherm. The adsorption capacity was tested using the methyl orange and the result was almost 100% removal efficiency at an adsorbent dose of 2 g·L^{-1} and initial concentration of 100 mg·L^{-1}. The results demonstrated that the obtained activated carbon is effective for removing dyes from aqueous solution.

Data Availability

The data used to support the findings of this study are included within the article.

Conflicts of Interest

The authors declare that they have no conflicts of interest.

Acknowledgments

We are grateful to the Center of Analyses and Characterization (CAC) of University Caddy Ayyad, Morocco. Also, our respectful thanks go to professors of REMATOP, LCOA, and REMINEX Managem laboratories in Marrakech, Morocco.

References

[1] K. Ennaciri, A. Baçaoui, M. Sergent, and A. Yaacoubi, "Application of fractional factorial and Doehlert designs for optimizing the preparation of activated carbons from Argan shells," *Chemometrics and Intelligent Laboratory Systems*, vol. 139, pp. 48–57, 2014.

[2] R. Salemdeeb, E. K. H. J. zu Ermgassen, M. H. Kim, A. Balmford, and A. Al-tabbaa, "Environmental and health impacts of using food waste as animal feed: a comparative analysis of food waste management options," *Journal of Cleaner Production*, vol. 140, pp. 871–880, 2017.

[3] D. S. Martin, S. Ramos, and J. Zufía, "Valorisation of food waste to produce new raw materials for animal feed," *Food Chemistry*, vol. 198, pp. 68–74, 2016.

[4] C. Du, J. J. Abdullah, D. Greetham et al., "Valorization of food waste into biofertiliser and its field application," *Journal of Cleaner Production*, vol. 187, pp. 273–284, 2018.

[5] A. Cerda, A. Artola, X. Font, R. Barrena, T. Gea, and A. Sánchez, "Composting of food wastes: status and challenges," *Bioresource Technology*, vol. 248, pp. 57–67, 2018.

[6] C. I. A. Ferreira, V. Calisto, E. M. Cuerda-correa, M. Otero, H. Nadais, and V. I. Esteves, "Comparative valorisation of agricultural and industrial biowastes by combustion and pyrolysis," *Bioresource Technology*, vol. 218, pp. 918–925, 2016.

[7] D. Marcelo, W. Bizzo, M. Alamo, and E. Vásquez, "Assessment of sugarcane byproducts for energy use in Peru," *Energy Procedia*, vol. 115, pp. 397–408, 2017.

[8] M. Sharma and A. Kumar, "Promising biomass materials for biofuels in India's context," *Materials Letters*, vol. 220, pp. 175–177, 2018.

[9] P. K. Swain, "Utilisation of agriculture waste products for production of bio-fuels: a novel study," *Materials Today: Proceedings*, vol. 4, no. 11, pp. 11959–11967, 2017.

[10] N. Mohamed, R. Othman, N. M. Mubarak, and E. Chan, "Agricultural biomass-derived magnetic adsorbents: preparation and application for heavy metals removal," *Journal of the Taiwan Institute of Chemical Engineers*, vol. 78, pp. 168–177, 2017.

[11] P. N. Omo-okoro, A. P. Daso, and J. O. Okonkwo, "A review of the application of agricultural wastes as precursor materials for the adsorption of per- and polyfluoroalkyl substances: a focus on current approaches and methodologies," *Environmental Technology and Innovation*, vol. 9, pp. 100–114, 2018.

[12] Y. El maguana, N. Elhadiri, M. Bouchdoug, and M. Benchanaa, "Study of the influence of some factors on the preparation of activated carbon from walnut cake using the fractional factorial design," *Journal of Environmental Chemical Engineering*, vol. 6, no. 1, pp. 1093–1099, 2018.

[13] D. Adinata, W. Wandaud, and M. Aroua, "Preparation and characterization of activated carbon from palm shell by chemical activation with K2CO3," *Bioresource Technology*, vol. 98, no. 1, pp. 145–149, 2007.

[14] J. Yang and K. Qiu, "Preparation of activated carbons from walnut shells via vacuum chemical activation and their application for methylene blue removal," *Chemical Engineering Journal*, vol. 165, no. 1, pp. 209–217, 2010.

[15] S. M. Yakout and G. Sharaf El-Deen, "Characterization of activated carbon prepared by phosphoric acid activation of olive stones," *Arabian Journal of Chemistry*, vol. 9, pp. S1155–S1162, 2016.

[16] A. Moubarik and N. Grimi, "Valorization of olive stone and sugar cane bagasse by-products as biosorbents for the removal of cadmium from aqueous solution," *Food Research International*, vol. 73, pp. 169–175, 2015.

[17] A. L. Cazetta, A. M. M. Vargas, E. M. Nogami et al., "NaOH-activated carbon of high surface area produced from coconut shell: kinetics and equilibrium studies from the methylene blue adsorption," *Chemical Engineering Journal*, vol. 174, no. 1, pp. 117–125, 2011.

[18] K. Y. Foo and B. H. Hameed, "Mesoporous activated carbon from wood sawdust by K2CO3 activation using microwave heating," *Bioresource Technology*, vol. 111, pp. 425–432, 2012.

[19] A. Elmouwahidi, Z. Zapata-Benabithe, F. Carrasco-Marín, and C. Moreno-Castilla, "Activated carbons from KOH-activation of argan (Argania spinosa) seed shells as supercapacitor electrodes," *Bioresource Technology*, vol. 111, pp. 185–190, 2012.

[20] W. C. Lim, C. Srinivasakannan, and N. Balasubramanian, "Activation of palm shells by phosphoric acid impregnation for high yielding activated carbon," *Journal of Analytical and Applied Pyrolysis*, vol. 88, no. 2, pp. 181–186, 2010.

[21] B. S. Girgis and A.-N. A. El-Hendawy, "Porosity development in activated carbons obtained from date pits under chemical activation with phosphoric acid," *Microporous and Mesoporous Materials*, vol. 52, no. 2, pp. 105–117, 2002.

[22] N. Barka, K. Ouzaouit, M. Abdennouri, and M. E. Makhfouk, "Dried prickly pear cactus (Opuntia ficus indica) cladodes as a low-cost and eco-friendly biosorbent for dyes removal from aqueous solutions," *Journal of the Taiwan Institute of Chemical Engineers*, vol. 44, no. 1, pp. 52–60, 2013.

[23] L. Hassini, E. Bettaieb, H. Desmorieux, S. S. Torres, and A. Touil, "Desorption isotherms and thermodynamic properties of prickly pear seeds," *Industrial Crops and Products*, vol. 67, pp. 457–465, 2015.

[24] R. Kumar and M. A. Barakat, "Decolourization of hazardous brilliant green from aqueous solution using binary oxidized cactus fruit peel," *Chemical Engineering Journal*, vol. 226, pp. 377–383, 2013.

[25] D. Prahas, Y. Kartika, N. Indraswati, and S. Ismadji, "Activated carbon from jackfruit peel waste by H3PO4 chemical activation: pore structure and surface chemistry characterization," *Chemical Engineering Journal*, vol. 140, no. 1-3, pp. 32–42, 2008.

[26] S. Yorgun and D. Yıldız, "Preparation and characterization of activated carbons from Paulownia wood by chemical activation with H3PO4," *Journal of the Taiwan Institute of Chemical Engineers*, vol. 53, pp. 122–131, 2015.

[27] H. Tounsadi, A. Khalidi, M. Abdennouri, and N. Barka, "Activated carbon from Diplotaxis Harra biomass: optimization of preparation conditions and heavy metal removal," *Journal of the Taiwan Institute of Chemical Engineers*, vol. 59, pp. 348–358, 2016.

[28] M. Danish, R. Hashim, M. N. M. Ibrahim, and O. Sulaiman, "Optimization study for preparation of activated carbon from Acacia mangium wood using phosphoric acid," *Wood Science and Technology*, vol. 48, no. 5, pp. 1069–1083, 2014.

[29] M. K. B. Gratuito, T. Panyathanmaporn, R.-A. Chumnanklang, N. Sirinuntawittaya, and A. Dutta, "Production of activated carbon from coconut shell: optimization using response surface methodology," *Bioresource Technology*, vol. 99, no. 11, pp. 4887–4895, 2008.

[30] M. A. Nahil and P. T. Williams, "Pore characteristics of activated carbons from the phosphoric acid chemical activation of cotton stalks," *Biomass and Bioenergy*, vol. 37, pp. 142–149, 2012.

[31] K. Legrouri, M. El Harti, M. Oumam et al., "Characterization and evaluation performance of activated carbon prepared from coconut shell argan," *Journal of Chemical and Pharmaceutical Research*, vol. 4, no. 12, pp. 5081–5088, 2012.

[32] A. Omri, M. Benzina, and N. Ammar, "Preparation, modification and industrial application of activated carbon from almond shell," *Journal of Industrial and Engineering Chemistry*, vol. 19, no. 6, pp. 2092–2099, 2013.

[33] R. Baccar, M. Sarrà, J. Bouzid, M. Feki, and P. Blánquez, "Removal of pharmaceutical compounds by activated carbon prepared from agricultural by-product," *Chemical Engineering Journal*, vol. 211-212, pp. 310–317, 2012.

[34] A. Baçaoui, A. Yaacoubi, A. Dahbi et al., "Optimization of conditions for the preparation of activated carbons from olive-waste cakes," *Carbon*, vol. 39, no. 3, pp. 425–432, 2001.

[35] P. Patnukao and P. Pavasant, "Activated carbon from *Eucalyptus camaldulensis* Dehn bark using phosphoric acid

activation," *Bioresource Technology*, vol. 99, no. 17, pp. 8540–8543, 2008.

[36] Y. El maguana, N. Elhadiri, M. Bouchdoug, M. Benchanaa, and A. Boussetta, "Optimization of preparation conditions of novel adsorbent from sugar scum using response surface methodology for removal of methylene blue," *Journal of Chemistry*, vol. 2018, Article ID 2093654, 10 pages, 2018.

[37] S. Nejjar, H. El Moussami, S. Dahbi, and L. Ezzine, "Optimisation du contrcôle géométrique des tubes cintrés du système de freinage," in *Proceedings of Xème Conférence Internationale : conception et production intégrées*, Tanger, Morocco, December 2015.

[38] T. Santhi and S. Manonmani, "Removal of methylene blue from aqueous solution by bioadsorption onto *Ricinus communis* epicarp activated carbon," *Chemical Engineering Research Bulletin*, vol. 13, no. 1, pp. 1–5, 2009.

[39] A. A. Attia, B. S. Girgis, and S. A. Khedr, "Capacity of activated carbon derived from pistachio shells by H3PO4 in the removal of dyes and phenolics," *Journal of Chemical Technology and Biotechnology*, vol. 78, no. 6, pp. 611–619, 2003.

[40] D. Li, J. Yan, Z. Liu, and Z. Liu, "Adsorption kinetic studies for removal of methylene blue using activated carbon prepared from sugar beet pulp," *International Journal of Environmental Science and Technology*, vol. 13, no. 7, pp. 1815–1822, 2016.

[41] H. Deng, G. Zhang, X. Xu, G. Tao, and J. Dai, "Optimization of preparation of activated carbon from cotton stalk by microwave assisted phosphoric acid-chemical activation," *Journal of Hazardous Materials*, vol. 182, no. 1-3, pp. 217–224, 2010.

[42] Ü. Geçgel, G. Özcan, and G. Ç. Gürpınar, "Removal of sethylene blue from aqueous solution by activated carbon prepared from pea shells (*Pisum sativum*)," *Journal of Chemistry*, vol. 2013, Article ID 614083, 9 pages, 2013.

[43] Ü. Geçgel, B. Kocabıyık, and O. Üner, "Adsorptive removal of methylene blue from aqueous solution by the activated carbon obtained from the fruit of catalpa bignonioides," *Water, Air, and Soil Pollution*, vol. 226, no. 8, 2015.

[44] O. S. Diallo and R. Mathis, "Etude en spectrographie infrarouge et de résonance magnétique nucléaire de l'hydrolyse et de l'acidolyse d'un amido-phosphite bicyclique contraint," *Spectrochimica Acta Part A: Molecular Spectroscopy*, vol. 39, no. 2, pp. 153–157, 1983.

[45] J. M. Salman, "Optimization of preparation conditions for activated carbon from palm oil fronds using response surface methodology on removal of pesticides from aqueous solution," *Arabian Journal of Chemistry*, vol. 7, no. 1, pp. 101–108, 2014.

[46] M. M. Hamed, I. M. Ahmed, and S. S. Metwally, "Adsorptive removal of methylene blue as organic pollutant by marble dust as eco-friendly sorbent," *Journal of Industrial and Engineering Chemistry*, vol. 20, no. 4, pp. 2370–2377, 2014.

[47] K. Haddad, S. Jellali, S. Jaouadi, and M. Benltifa, "Raw and treated marble wastes reuse as low cost materials for phosphorus removal from aqueous solutions: efficiencies and mechanisms," *Comptes Rendus Chimie*, vol. 18, no. 1, 2014.

[48] M. A. Martín-González, P. Susial, J. Pérez-Peña, and J. M. Doña-Rodríguez, "Preparation of activated carbons from banana leaves by chemical activation with phosphoric acid. Adsorption of methylene blue," *Revista Mexicana de Ingeniería Química*, vol. 12, no. 3, pp. 595–608, 2013.

[49] D. Zhang, H. Luo, L. Zheng et al., "Utilization of waste phosphogypsum to prepare hydroxyapatite nanoparticles and its application towards removal of fluoride from aqueous solution," *Journal of Hazardous Materials*, vol. 241-242, pp. 418–426, 2012.

[50] Y. X. Wang, H. H. Ngo, and W. S. Guo, "Preparation of a specific bamboo based activated carbon and its application for ciprofloxacin removal," *Science of the Total Environment*, vol. 533, pp. 32–39, 2015.

[51] D. Mehta, P. Mondal, and S. George, "Utilization of marble waste powder as a novel adsorbent for removal of fluoride ions from aqueous solution," *Journal of Environmental Chemical Engineering*, vol. 4, no. 1, pp. 932–942, 2016.

[52] S. Gao, R. Sun, Z. Wei, H. Zhao, H. Li, and F. Hu, "Size-dependent defluoridation properties of synthetic hydroxyapatite," *Journal of Fluorine Chemistry*, vol. 130, no. 6, pp. 550–556, 2009.

[53] E. C. Lima, A. Hosseini-Bandegharaei, J. C. Moreno-Piraján, and I. Anastopoulos, "A critical review of the estimation of the thermodynamic parameters on adsorption equilibria. Wrong use of equilibrium constant in the Van't Hoof equation for calculation of thermodynamic parameters of adsorption," *Journal of Molecular Liquids*, vol. 273, pp. 425–434, 2019.